

Hollow Zeolitic Imidazolate Framework Nanospheres as Highly Efficient Cooperative Catalysts for [3+3] Cycloaddition Reactions

Fang Zhang,^{†,‡} Yongyi Wei,^{†,‡} Xiaotao Wu,[†] Huangyong Jiang,[†] Wei Wang,^{*,‡} and Hexing Li^{*,†}

[†]The Education Ministry Key Laboratory of Resource Chemistry and Shanghai Key Laboratory of Rare Earth Functional Materials, Shanghai Normal University, Shanghai 200234, China

[‡]Department of Chemistry & Chemical Biology, University of New Mexico, Albuquerque, New Mexico 87131-0001, United States

S Supporting Information

ABSTRACT: Herein we describe a novel, hollow-structured zeolitic imidazolate framework (ZIF-8-H) nanosphere as a highly efficient catalyst for [3+3] cycloaddition reactions. The programmed installation of acidic Zn²⁺ species and basic imidazolate moieties creates a synergistic catalytic system. Appropriate positioning of these functionalities in the catalytic system makes it possible to bring two substrates into close proximity and activate them cooperatively. Moreover, the flexible shell and the surface mesopores of ZIF-8-H provide the capacity for favorable binding of various sized substrates, stabilizing intermediates via their multiple force networks and the increased accessibility of the active sites. These features render ZIF-8-H a more highly active promoter than its homogeneous precursors, bulk ZIF-8 and ZIF-8-N nanoparticles. Finally, the robust catalyst can be easily recovered and reused 10 times without loss of catalytic activity.

Despite intensive efforts to synthesize heterogeneous catalysts by incorporating various functionalities into nanostructures to mimic an enzyme,¹ achieving a level of catalytic efficiency with a synthetic catalyst similar to that of an enzyme is still a significant challenging task. It is easy for an artificial catalyst to lower the activation energy of the reaction but exceedingly difficult to endow it with the additional catalytic features enzymes possess,² such as correct positioning of appropriate functional groups of the enzyme on the substrate, selective binding of the substrate via multiple forces, the right size of substrate fitting in the enzyme active site for optimal activation and reactivity, and favorable binding of substrates over products,^{3,4} in a cooperative manner.⁵ Therefore, the construction of additional binding and regulating features around the catalytic center with correct positioning is critical but would certainly demand sophisticated design and synthesis.

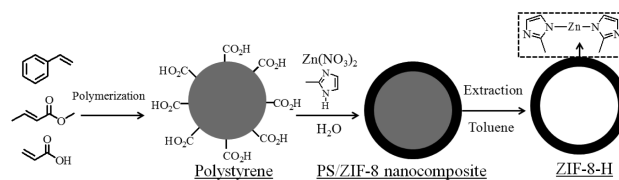
Metal–organic frameworks (MOFs) are porous crystalline materials constituted by metal species and polyfunctional organic linkers in a defined pattern. Their unique properties place these nanostructures at the frontier between zeolites and enzymes.⁶ One unrivaled feature of MOF materials is that functional groups can be positioned at precise distances relative to one another. Zeolitic imidazolate frameworks (ZIFs) are a particularly appealing class of MOFs for catalysis application because of their high thermal and chemical stability.⁷ ZIF-based catalysts

have been explored in simple organic transformations such as transesterification⁸ and Knoevenagel reactions,⁹ simply by employing their Lewis acid or base features. Nevertheless, the utilization of their powerful capability in the installation of functional groups to craft synthetic catalysts in a synergistic fashion has been slow to emerge.¹⁰ Moreover, the use of ZIFs as catalysts in promoting organic transformations involving multiple-step reactions to efficiently construct complex molecule structures has not been explored.

Herein we report a facile approach to construct a hollow-structured ZIF-8 nanosphere (ZIF-8-H) as an efficient heterogeneous catalyst for [3+3] cycloaddition reactions to give synthetically valuable pyranil heterocycles¹¹ for the first time. It exhibits higher catalytic efficiency than homogeneous precursors Zn(NO₃)₂ and 2-methylimidazole (2-MIM) or bulk ZIF-8 and ZIF-8-N nanoparticles. The synergistic acid–base catalytic effect arising from the proper positioning of Zn(II) and imidazolate functional groups in ZIF-8-H makes it possible to bring two substrates in close proximity and activate them cooperatively through multiple interactions. Moreover, the flexible shell and the surface mesopores enable favorable binding of various sized substrates over products and stabilizing intermediates (for a proposed reaction mechanism, see Figure S1). Finally, like a typical heterogeneous catalyst, the robust ZIF-8-H can be readily recycled by simple filtration and subsequently reused without significant loss of its catalytic activity in a 10 times run test.

The synthesis of ZIF-8-H is illustrated in Scheme 1 (for detailed procedure, see SI). Briefly, carboxylate-terminated

Scheme 1. Illustration of the Preparation of ZIF-8-H



polystyrene (PS) nanospheres with a diameter of 400 nm were prepared according to a previously reported procedure.¹² Coordination of HOOC groups on the surface of the PS nanospheres with Zn ions and 2-methylimidazole then initiated the growth of ZIF-8, leading to the formation of a PS/ZIF-8

Received: June 25, 2014

Published: September 25, 2014

nanocomposite. Finally, the PS cores were removed by immersing in toluene to give ZIF-8-H.^{13a} The FT-IR spectrum of ZIF-8-H revealed that the characteristic peaks of the phenyl ring at 698, 1449, 1492, and 1602 cm^{-1} in PS had disappeared (Figure S2), indicating the complete removal of PS.^{13b} In parallel, the control bulk nonspherical ZIF-8 and ZIF-8-N nanoparticles without PS as template were synthesized in aqueous solution by using the same precursors.

Figure 1a shows a scanning electron microscopy (SEM) image of the synthesized ZIF-8-H. The formation of isolated spheres in

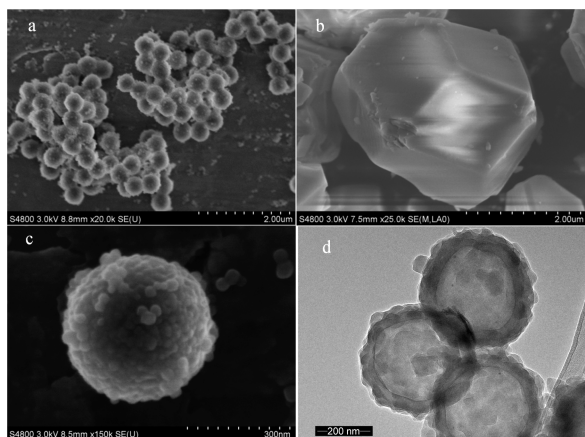


Figure 1. SEM images of ZIF-8-H (a) and ZIF-8 (b). High-resolution SEM (c) and TEM (d) pictures of ZIF-8-H.

large domains with a nearly uniform size around 500 nm is observed, while bulk ZIFs display irregular morphology with the average diameter $>3.0 \mu\text{m}$ (Figure 1b). In comparison with the PS template (Figure S3), a high-resolution SEM picture reveals the increasing diameter of ZIF-8-H, with formation of nanosized crystals on the surface (Figure 1c). The increased size was confirmed by dynamic light scattering analysis (Figure S4). The PS nanosphere precursors have an apparent hydrodynamic radius of 410 nm, while that of ZIF-8-H is about 515 nm, indicating the average size of the newly formed surface nanocrystals is about 50 nm. It is noteworthy that the amount of PS template employed is critical for the morphology of the nanostructure. Either a decreased (25 mg) or an increased (200 mg) amount did not generate the intact core-shell structured PS/ZIF-8 nanocomposite, instead resulting in nonuniform hollow nanospheres (Figure S5). The uniformly spherical hollow morphology of ZIF-8-H was further characterized by transmission electron microscopy (TEM) analysis (Figure 1d). The obtained ZIF-8-N nanoparticles of about 60 nm size were confirmed by SEM and TEM images (Figure S6).

The composition of the shell was analyzed by X-ray diffraction (XRD) measurement (Figure S7a), which revealed that ZIF-8-H maintains well-resolved diffraction peaks similar to those of bulk ZIF-8, indicating that the shell is composed of ZIF-8 materials.¹⁴ However, the XRD peaks are relatively weak and broad, which is consistent with the ZIF-8-N, indicating the formation of crystalline-sized ZIF-8 at the nanoscale. ZIF-8, ZIF-8-H, and ZIF-8-N display type I N_2 adsorption-desorption isotherms (Figure S7b). The increase in the volume adsorbed at very low relative pressure ($P/P_0 = 0.05$) arises from the presence of micropores. For ZIF-8-N, an additional uptake at high relative pressure around $P/P_0 = 0.9$ reveals the existence of textural pores formed by packing of nanoparticles.¹⁵ Interestingly, ZIF-8-H has

a slight adsorption at $P/P_0 = 0.45$, suggesting the presence of some mesopores.^{2b} Moreover, it has a large hysteresis loop at high pressure, which could be ascribed to the emptying of the large internal cavity.¹⁶ In addition, in comparison with the BET surface areas of bulk ZIF-8 (1017 m^2/g) and ZIF-8-N nanoparticles (1003 m^2/g), no significant decrease in specific surface area was observed in ZIF-8-H (908 m^2/g), indicative of the microporous shell feature.

As discussed above, the versatile, unique ZIF-8-H is designed to promote a [3+3] cycloaddition reaction with 1,3-cyclohexanediones and enals. The hollow nanostructure with programmed positioning of acidic and basic functionalities makes it possible to bring two substrates in close proximity and simultaneously activate them. Moreover, the relatively nonpolar products should prefer the nonpolar solvent instead of the hydrophilic ZIF-8-H, vacating the binding site(s) for new substrates to come in. Therefore, it is expected that ZIF-8-H acts as an efficient nanoreactor in substrate binding and product turnover. Although the reaction has been demonstrated in homogeneous catalysis with either base or acid catalysts,¹¹ it is difficult to employ dual acid-base catalysis in a homogeneous system due to acid-base interference, as demonstrated in our studies (see below).

Reaction of 1,3-cyclohexanedione with 3-methyl-2-butenal was used to probe the catalytic performance of ZIF-8-H catalyst (Table 1). Indeed, ZIF-8-H displayed high catalytic efficiency

Table 1. Catalytic Properties of Different Catalysts in [3+3] Cycloaddition Reactions between 1,3-Cyclohexanedione and α,β -Unsaturated Aldehydes^a

Entry	Catalyst	Aldehyde	Product	Conv. (%)	Sel. (%)
1	ZIF-8-H			89.0	99.9
2	$\text{Zn}(\text{NO}_3)_2$			44.5	80.0
3	2-MIM ^b			73.6	99.9
4	$\text{Zn}(\text{NO}_3)_2$ + 2-MIM ^c			15.9	85.5
5	ZIF-8			73.2	99.9
6	ZIF-8-N			81.0	99.9
7	ZIF-8-H-c ^d			81.6	99.9
8	ZIF-8-H			76.7	99.9
9	ZIF-8			54.3	99.9
10	ZIF-8-N			68.4	99.9
11	ZIF-8-H			65.4	99.9
12	ZIF-8			33.8	99.9
13	ZIF-8-N			58.6	99.9
14	ZIF-8-H			63.3	99.9
15	ZIF-8			32.8	99.9
16	ZIF-8-N			57.2	99.9
17	ZIF-8-H			50.2	91.0
18	ZIF-8			24.1	91.7
19	ZIF-8-N			43.9	91.5

^aReaction conditions: 50 mg of ZIF-8-H, ZIF-8, ZIF-8-N, $\text{Zn}(\text{NO}_3)_2$, or 2-MIM, 1.0 mmol dione, 1.0 mmol aldehyde, 5.0 mL of CH_2Cl_2 , $T = 20^\circ\text{C}$, $t = 24 \text{ h}$. ^b34–86% yields obtained using amine catalyst (see ref 11k). ^c17 mg of $\text{Zn}(\text{NO}_3)_2$ and 33 mg of 2-methylimidazole. ^dAfter ball-milling for 0.5 h (500 rpm).

under mild reaction conditions (89% conversion and 99.9% selectivity, entry 1). However, in parallel studies homogeneous acid $\text{Zn}(\text{NO}_3)_2$ (entry 2) and basic 2-methylimidazole (2-MIM, entry 3) exhibited poorer catalytic performance. Furthermore, the employment of a mixture of $\text{Zn}(\text{NO}_3)_2$ and 2-MIM as dual acid–base catalysts gave unsatisfactory results (entry 4): only 15.9% conversion and 85.5% selectivity were observed. This may be due to the difficulty of manipulating the positioning of the active species, thus inducing acid–base interference in a homogeneous system.^{17,18} Since the use of ZIF-8 as the basic catalyst has been studied,⁹ we used temperature-programmed desorption (TPD) of ammonia to confirm the existence of acidic sites in ZIF-8-H as a cocatalyst (Figure S8).¹⁹ Besides the desorption peak in the temperature range from 280 to 550 °C due to the decomposition of organic compounds in ZIF-8-H, TPD displayed a NH_3 desorption peak center at 208 °C, implying the presence of weak acid sites in ZIF-8-H. Furthermore, we compared the catalytic activity of ZIF-8-H and ZIF-8-N in the reactions (entries 6, 10, 16, and 19) and found that ZIF-8-N exhibited slightly poorer catalytic efficiency than ZIF-8-H. Moreover, a crushed ZIF-8-H sample was prepared by ball-milling treatment and tested for catalysis (entry 7 vs entry 1). It was inferior to that of intact ZIF-8-H as a result of the change from the hollow structure to dispersed nanoparticles based on the TEM image (Figure S9). We also examined the catalytic activity of bulk ZIF-8 (Table 1, entry 5) and found that a lower catalytic efficiency was observed. X-ray photoelectron spectra revealed that all N and Zn species in ZIF-8-H and ZIF-8 were present in the same electronic state (Figure S10), indicative of their similar chemical microenvironment. Furthermore, thermogravimetry–differential thermal analysis of a ZIF-8-H sample confirmed that PS templates were removed completely, since it had weight-loss curve similar to that of ZIF-8 (Figure S11). The inferior catalytic performance of ZIF-8 in comparison with ZIF-8-H suggests that the increased catalytic efficiency ZIF-8-H must be related to its unique hollow structure.

To explain this phenomenon, we first conducted a vapor-phase adsorption study of toluene in ZIF-8-H.²⁰ Surprisingly, ZIF-8-H can adsorb toluene to a cage-filling level with high adsorption amount (6.34 mmol/g, Figure 2a). This implies that the limiting

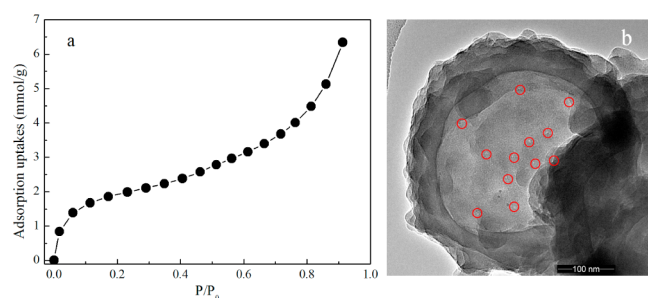


Figure 2. Toluene vapor adsorption isotherm (a) and high-resolution TEM image (b) of ZIF-8-H.

aperture size of ZIF-8-H exceeds the kinetic diameter of toluene (0.61 nm), which is much larger than the reported window size (0.34 nm) of ZIF-8.²¹ This result supports the observation that relatively large reactants are able to diffuse into the internal micropores of ZIF-8-H.²² In addition, its high-resolution TEM image (Figure 2b) confirmed that the mesopores (marked with red circles) could be clearly found on the surface of ZIF-8-H. We believe that these mesopores were mainly produced from

stacking of the nanocrystals.²³ Overall, it can be concluded that this nanocatalytic vehicle possesses the flexible shell and the mesopores to efficiently facilitate the accommodation and diffusion of the various sized substrates,²⁴ and the increased accessibility of active sites resulting from the anti-aggregation and low density properties.²⁵ These features lead to the enhanced catalytic activity of ZIF-8-H compared to bulk ZIF-8 and ZIF-8-N. Indeed, the structural characteristics that endow the high catalytic behavior are reflected in the tolerance of different sized α,β -unsaturated aldehydes (Table 1, entries 8–19, and Table 2)

Table 2. Catalytic Properties of ZIF-8-H, ZIF-8, and ZIF-8-N in [3+3] Cycloaddition Reactions between 4-Pyran-3,6-dione and α,β -Unsaturated Aldehydes^a

Entry	Catalyst	Aldehyde	Product	Conv. (%)	Sel. (%)
1	ZIF-8-H			73.5	99.9
2	ZIF-8			55.7	99.9
3	ZIF-8-N			69.4	99.9
4	ZIF-8-H			68.3	99.9
5	ZIF-8			43.2	99.9
6	ZIF-8-N			62.3	99.9
7	ZIF-8-H			52.8	99.9
8	ZIF-8			28.2	99.9
9	ZIF-8-N			46.2	99.9
10	ZIF-8-H			47.5	99.9
11	ZIF-8			23.9	99.9
12	ZIF-8-N			41.7	99.9
13	ZIF-8-H			39.4	90.2
14	ZIF-8			16.6	91.5
15	ZIF-8-N			34.7	91.0

^aReaction conditions are given in Table 1.

and 4-pyran-3,6-dione (Table 2). These results clearly demonstrate the advantage and capacity of the hollow-structured MOF for efficient catalytic synthesis of structurally diverse and functionalized molecules.

To determine whether the heterogeneous or the dissolved Zn(II) and/or N active sites were the real catalyst responsible for the [3+3] cycloaddition reaction, the following step was carried out according to the procedure proposed by Sheldon et al.²⁶ After reaction for 10 h with the conversion exceeding 40%, the solid catalyst was filtered, and the mother liquor was allowed to react for another 12 h under the same conditions. No significant change in either the conversion or the product yield was detected, indicating that the reaction indeed occurred due to ZIF-8-H rather than dissolved Zn(II) and/or N active sites.

Finally, the heterogeneous ZIF-8-H catalyst was proved to be a robust promoter for the [3+3] cycloaddition process, using 1,3-cyclohexanedione and 3-methyl-2-butenal as examples (Figure S12). ZIF-8-H could be recycled and reused at least 10 times without losing its original activity. The XRD pattern and TEM image (Figure S13) of the recycled ZIF-8-H were consistent with those of the as-prepared one.

In summary, we have developed a new hollow-structured ZIF-8-H nanosphere as an efficient catalyst for [3+3] cycloaddition reactions. This is the first example demonstrating the use of ZIF as promoter for a cascade process to facilitate assembly of an array of

synthetically useful molecules. The heterogeneous promoter is easily constructed. It displays unique catalytic behavior with high catalytic efficiency by virtue of cooperative interactions and activation and favorable binding of substrates over products. Furthermore, the nanostructures can be recycled and reused at least 10 times without loss of activity. Further exploration of the strategy and application of the heterogeneous system in new organic transformations are being pursued in our laboratories.

■ ASSOCIATED CONTENT

■ Supporting Information

Catalyst preparation; procedures for catalytic reactions; characterization of MOFs. This material is available free of charge via the Internet at <http://pubs.acs.org>.

■ AUTHOR INFORMATION

Corresponding Authors

wwang@unm.edu
hexing-li@shnu.edu.cn

Notes

The authors declare no competing financial interest.

■ ACKNOWLEDGMENTS

This work is supported by the Natural Science Foundation of China (21107071 and 51273112), PCSIRT (IRT1269), and Shanghai Government (12CG52 and 13QA1402800).

■ REFERENCES

- (1) (a) Benaglia, M. *Recoverable and Recyclable Catalysts*; Wiley: Chichester, 2009. (b) Shylesh, S.; Wagener, A.; Seifert, A.; Ernst, S.; Thiel, W. R. *Angew. Chem., Int. Ed.* **2010**, *49*, 184. (c) Sakakura, B.; Kohno, K. *Chem. Commun.* **2009**, *11*, 1312. (d) Chi, Y.; Scroggins, S. T.; Fréchet, J. M. J. *J. Am. Chem. Soc.* **2008**, *130*, 6322. (e) Gu, Z.; Park, J.; Raiff, A.; Wei, Z. W.; Zhou, H. C. *ChemCatChem* **2014**, *6*, 67.
- (2) (a) Diaz, U.; Brunel, D.; Corma, A. *Chem. Soc. Rev.* **2013**, *42*, 4083. (b) Shylesh, S.; Thiel, W. R. *ChemCatChem* **2011**, *3*, 278. (c) Motokura, K.; Tada, M.; Iwasawa, Y. *J. Am. Chem. Soc.* **2007**, *129*, 9540. (d) Brunellis, N. A.; Didas, S. A.; Venkatasubbiah, K.; Jones, C. W. *J. Am. Chem. Soc.* **2012**, *134*, 13950. (e) Huang, Y. L.; Xu, S.; Lin, V. S. *Angew. Chem., Int. Ed.* **2011**, *50*, 661.
- (3) Grate, J. W.; Frye, G. C. In *Sensors Update*, Vol. 2; Baltes, H., Göpel, W., Hesse, J., Eds.; Wiley-VCH: Weinheim, 1996; pp 10–20.
- (4) Jencks, W. P. *Adv. Enzymol. Relat. Areas Mol. Biol.* **1975**, *43*, 219.
- (5) Margelefsky, E. L.; Zeidan, R. K.; Davis, M. E. *Chem. Soc. Rev.* **2008**, *37*, 1118.
- (6) (a) Farrusseng, D. *Metal–Organic Frameworks. Applications from Catalysis to Gas Storage*; Wiley: Weinheim, 2009. (b) Corma, A.; Garcia, H.; Xamena, F. X. L.-i. *Chem. Rev.* **2010**, *110*, 4606. (c) Yoon, M.; Srirambalaji, R.; Kim, K. *Chem. Rev.* **2012**, *112*, 1196. (d) Lee, J. Y.; Farha, O. K.; Roberts, J.; Scheidt, K. A.; Nguyen, S. T.; Hupp, J. T. *Chem. Soc. Rev.* **2009**, *38*, 1450. (e) Ma, L.; Abney, C.; Lin, W. *Chem. Soc. Rev.* **2009**, *38*, 1248. (f) Zhu, C.; Yuan, G.; Chen, X.; Yang, Z.; Cui, Y. *J. Am. Chem. Soc.* **2012**, *134*, 8058. (g) Feng, D.; Gu, Z.; Li, J.; Jiang, H.; Wei, Z.; Zhou, H. *Angew. Chem., Int. Ed.* **2012**, *51*, 10307. (h) Roberts, J. M.; Fini, B. M.; Sarjeant, A. A.; Farha, O. K.; Hupp, J. T.; Scheidt, K. A. *J. Am. Chem. Soc.* **2012**, *134*, 3334. (i) Wu, P.; He, C.; Wang, J.; Peng, X.; Li, X.; An, Y.; Duan, C. *J. Am. Chem. Soc.* **2012**, *134*, 14991.
- (7) Park, K. S.; Ni, Z.; Côte, A. P.; Choi, J. Y.; Huang, R.; Uribe-Romo, F. J.; Chae, H. K.; O’Keeffe, M.; Yaghi, O. M. *Proc. Natl. Acad. Sci. U.S.A.* **2006**, *103*, 10186.
- (8) Chizallet, C.; Lazare, S.; Bazer-Bachi, D.; Bonnier, F.; Lecocq, V.; Soyer, E.; Quoineaud, A.-A.; Bats, N. *J. Am. Chem. Soc.* **2010**, *132*, 12365.
- (9) (a) Tran, U. P. N.; Le, K. K. A.; Phan, N. T. S. *ACS Catal.* **2011**, *1*, 120. (b) Zhou, X.; Zhang, H. P.; Wang, G. Y.; Yao, Z. G.; Tang, Y. R.; Zheng, S. S. *J. Mol. Catal. A* **2013**, *366*, 43. (c) Dhakshinamoorthy, A.; Opanasenko, M.; Čejka, J.; Garcia, H. *Adv. Synth. Catal.* **2013**, *355*, 247.

(d) Karagiari, O.; Lalonde, M. B.; Bury, W.; Sarjeant, A. A.; Farha, O. K.; Hupp, J. T. *J. Am. Chem. Soc.* **2012**, *134*, 18790.

(10) (a) Zhao, M.; Ou, S.; Wu, C. D. *Acc. Chem. Res.* **2013**, *47*, 1199. (b) Park, J.; Li, J. R.; Chen, Y. P.; Yu, J.; Yakovenko, A. A.; Wang, Z. U.; Sun, L. B.; Balbuena, P. B.; Zhou, H. C. *Chem. Commun.* **2012**, *48*, 9995.

(11) Hsung et al. pioneered the homogeneous catalytic [3+3] cycloaddition reactions. For a review, see: (a) Buchanan, G. S.; Feltenberger, J. B.; Hsung, R. P. *Curr. Org. Synth.* **2010**, *7*, 363. For selected examples, see: (b) Buchanan, G. S.; Dai, H.; Hsung, R. P.; Gerasuto, A. I.; Scheinebeck, C. M. *Org. Lett.* **2011**, *13*, 4402. (c) Gerasuto, A. I.; Hsung, R. P. *J. Org. Chem.* **2007**, *72*, 2476. (d) Kurdyumov, A. V.; Lin, N.; Hsung, R. P.; Gullickson, G. C.; Cole, K. P.; Sydorenko, N.; Swidorski, J. *J. Org. Lett.* **2006**, *8*, 191. (e) Gerasuto, A. I.; Hsung, R. P.; Sydorenko, N.; Slafer, B. *J. Org. Chem.* **2005**, *70*, 4248. (f) Sydorenko, N.; Hsung, R. P.; Darwish, O. S.; Hahn, J. M.; Liu, J. *J. Org. Chem.* **2004**, *69*, 6732. (g) Cole, K. P.; Hsung, R. P. *Org. Lett.* **2003**, *5*, 4843. (h) Luo, S.; Zifcick, C. A.; Hsung, R. P. *Org. Lett.* **2003**, *5*, 4709. (i) Sklenicka, H. M.; Hsung, R. P.; McLaughlin, M. J.; Wei, L. L.; Gerasuto, A. I.; Brennessel, W. B. *J. Am. Chem. Soc.* **2002**, *124*, 10435. (j) Wei, L. L.; Hsung, R. P.; Sklenicka, H. M.; Gerasuto, A. I. *Angew. Chem., Int. Ed.* **2001**, *40*, 1516. (k) Hsung, R. P.; Shen, H. C.; Douglas, C. J.; Morgan, C. D.; Degen, S. J.; Yao, L. J. *J. Org. Chem.* **1999**, *64*, 690. (l) Fang, X.; Li, J.; Tao, H.-Y.; Wang, C.-J. *Org. Lett.* **2013**, *15*, 5554. (m) Tong, M.-C.; Chen, X.; Tao, H.-Y.; Wang, C.-J. *Angew. Chem., Int. Ed.* **2013**, *52*, 12377.

(12) (a) Haes, A. J.; Hall, W. P.; Chang, L.; Klein, W. L.; Duyne, R. P. *Van Nano Lett.* **2004**, *4*, 1029. (b) Carné-Sánchez, A.; Imaz, I.; Cano-Sarabia, M.; MasPOCH, D. *Nat. Chem.* **2013**, *5*, 203. (c) Lee, H. J.; Cho, W.; Oh, M. *Chem. Commun.* **2012**, *48*, 221.

(13) (a) Imhof, A. *Langmuir* **2001**, *17*, 3579. (b) Yin, Y.; Chen, M.; Zhou, S.; Wu, L. *J. Mater. Chem.* **2012**, *22*, 11245.

(14) Jin, R. Z.; Bian, Z.; Li, J. Z.; Ding, M. X.; Gao, L. X. *Dalton Trans.* **2013**, *42*, 3936.

(15) Pan, Y. C.; Liu, Y. Y.; Zeng, G. F.; Zhao, L.; Lai, Z. P. *Chem. Commun.* **2011**, *47*, 2071.

(16) Jiang, X. M.; Ward, T. L.; Cheng, Y.; Liu, J. W.; Brinker, C. J. *Chem. Commun.* **2010**, *46*, 3019.

(17) Zhou, X.; Zhang, H. P.; Wang, G. Y.; Yao, Z. G.; Tang, Y. R.; Zhang, S. S. *J. Mol. Chem. A: Chem.* **2013**, *366*, 43.

(18) Žigon, M.; Šebenik, A.; Osredkar, U. *J. Appl. Polym. Sci.* **1992**, *45*, 597.

(19) Zhang, Z. J.; Xian, S. K.; Xi, H. X.; Wang, H. H.; Li, Z. *Chem. Eng. Sci.* **2011**, *66*, 4878.

(20) Zhang, K.; Lively, R. P.; Zhang, C.; Chance, R. R.; Koros, W. J.; Sholl, D. S.; Nair, S. *J. Phys. Chem. Lett.* **2013**, *4*, 3618.

(21) Wee, L. H.; Lescouet, T.; Ethiraj, J.; Bonino, F.; Vidruk, R.; Garrier, E.; Packet, D.; Bordiga, S.; Farrusseng, D.; Herskowitz, M.; Martens, J. A. *ChemCatChem* **2013**, *5*, 3562.

(22) (a) Farién-Jimenez, D.; Moggach, S. A.; Wharmby, M. T.; Wright, P. A.; Parsons, S.; Düren, T. *J. Am. Chem. Soc.* **2011**, *133*, 8900. (b) Kuo, C.; Tang, Y.; Chou, L.; Sneed, B. T.; Brodsky, C. N.; Zhao, Z.; Tsung, C. *J. Am. Chem. Soc.* **2012**, *134*, 14345.

(23) Wang, D. S.; Xie, T.; Peng, Q.; Li, Y. D. *J. Am. Chem. Soc.* **2008**, *130*, 4016.

(24) (a) Li, S. W.; Boucheron, T.; Tuel, A.; Farrusseng, D.; Meunier, F. *Chem. Commun.* **2014**, *50*, 1824. (b) Li, S. W.; Burel, L.; Aquino, C.; Tuel, A.; Meunier, F.; Rousset, J.; Farrusseng, D. *Chem. Commun.* **2013**, *49*, 8507.

(25) (a) Kim, S.; Kim, M.; Lee, W. Y.; Hyeon, T. *J. Am. Chem. Soc.* **2002**, *124*, 7672. (b) Li, H.; Lin, H.; Hu, Y.; Li, H. X.; Li, P.; Zhou, X. G. *J. Mater. Chem.* **2011**, *21*, 18447.

(26) Sheldon, R. A.; Wallau, M. I.; Arends, W. C. E.; Schuchardt, U. *Acc. Chem. Res.* **1998**, *31*, 485.